THE ASTROPHYSICAL JOURNAL, 498:728–734, 1998 May 10
© 1998. The American Astronomical Society. All rights reserved. Printed in U.S.A.

CLASSICAL AND QUANTUM-MECHANICAL CALCULATIONS OF $\mathrm{HCO}^+ + e \rightarrow \mathrm{CO}(v) + \mathrm{H}$

MAXIM TOMASHEVSKY
Department of Physics, Ohio State University, Columbus, Ohio 43210
ERIC HERBST
Departments of Physics and Astronomy, Ohio State University, Columbus, Ohio 43210-1106; herbst@ohstpy.mps.ohio-state.edu
AND
W. P. KRAEMER
Max-Planck-Institut für Physik und Astrophysik, Institut für Astrophysik, Karl-Schwarzschild-Strasse 1, D-85740 Garching, Germany
Received 1997 September 11; accepted 1997 December 16

ABSTRACT

It has been suggested that interstellar CO produced in the dissociative recombination between HCO^+ and electrons can be detected via infrared emission from excited vibrational levels. Using classical and quantum mechanical equations of motion, we have calculated the distribution of CO product vibrational states for the dissociative recombination reaction between HCO^+ and electrons. We have assumed the dissociation to occur along a purely linear geometry. The CO vibrational distribution has been calculated for two electronic states: (1) the ground $X\,^1\Sigma^+$ state and (2) the excited $a\,^3\Pi$ state. For the X state, we have used a newly calculated ab initio potential surface for the dissociation of HCO. Results for the a state can be compared with the results of experimental work by Adams and collaborators. Our results show that in general vibrational excitation of the CO product is not large, so that detection of infrared emission from interstellar clouds will not be facile.

Subject headings: ISM: abundances — ISM: clouds — ISM: molecules — molecular processes

1. INTRODUCTION

Dissociative recombination reactions play a key role in the ion-molecule chemistry of interstellar clouds (Herbst 1995). Although rate coefficients for this process have been studied in the laboratory for some time (Adams & Smith 1988; Mitchell 1990), it is only recently that the products of dissociative recombination reactions have begun to be measured (Adams et al. 1991; Adams 1992; Williams et al. 1996; Larsson, Lepp, & Dalgarno 1996; Vejby-Christensen et al. 1997). In addition to their importance in interstellar chemistry, dissociative recombination reactions deposit energy into clouds, both as product translational and product internal energy. Duley & Williams (1992) have suggested that vibrationally-excited interstellar CO, produced in the dissociative recombination between HCO^+ and electrons, can be detected by subsequent infrared emission.

Concurrently with the work on the detection of products, experimental and theoretical work has also been undertaken on the degree of vibrational excitation of the products of dissociative recombination reactions. In the laboratory, vibrational excitation in product OH was first detected (Herd, Adams, & Smith 1990). More recently, Adams & Babcock (1994) and Butler, Babcock, & Adams (1997) have studied the vibrational excitation of CO in its excited $a\,^3\Pi_r$ electronic state produced in the dissociative recombination of the ions HCO^+ and DCO^+ and the vibrational excitation of N_2 in its excited $B\,^3\Pi_g$ electronic state produced in the dissociative recombination of the ions HN_2^+ and DN_2^+.

In the realm of theory, Bates (1993) has developed and applied for HCO^+ a semiquantitative approach for the vibrational distribution of the products of dissociation recombination reactions. In his theory there are two distinct effects that can cause product vibrational excitation: (1) an *impulse* mechanism having to do with the impulse generated from a neighboring bond breaking along a repulsive potential curve, and (2) a *relic* mechanism in which an initial wave function for the local motion of a bond, averaged over the normal modes of the ion, is projected onto the final vibrational states.

According to the *impulse* mechanism, vibrational excitation is created by mutual repulsion between the separating products of recombination. The process is complete in a short time compared to the vibrational period, which allows the consideration of the repulsion as an instantaneous impulsive force. For linear HCO^+, this force causes a quick change in the relative momentum of C and O atoms of value δ, which is given by

$$\delta = \frac{m_{\mathrm{O}}}{m_{\mathrm{C}} + m_{\mathrm{O}}} \left(\frac{2 m_{\mathrm{H}} m_{\mathrm{C}} E}{m_{\mathrm{H}} + m_{\mathrm{C}}} \right)^{1/2} , \tag{1}$$

where E is the reaction exoergicity, and, correspondingly, a new wave function $\phi(p)$ for the C-O oscillator in the momentum representation of

$$\phi(p) = \psi_0(p + \delta) = \left(\frac{1}{\pi \alpha} \right)^{1/4} \exp \left[- \frac{(p + \delta)^2}{2\alpha} \right] , \tag{2}$$

where

$$\alpha = \frac{\mu_R \, \omega_{\mathrm{CO}}}{\hbar} , \tag{3}$$

μ_R is the C-O reduced mass, ω_{CO} is the angular harmonic frequency of CO, and ψ_0 represents the ground state C-O oscillator wave function in the ion. Then, assuming that the C-O equilibrium distance and force constant are the same in the molecule and in the ion, the probability of vibrational level v being excited is

$$P(v) = \left| \int_{-\infty}^{+\infty} \phi(p) \psi_v(p) dp \right|^2 , \tag{4}$$

which can be reduced to

$$P(v) = \frac{\lambda^{2v}}{2^v v!} \exp\left(-\frac{\lambda^2}{2}\right) , \tag{5}$$

$$\lambda = \delta/\alpha^{1/2} . \tag{6}$$

The vibrational population after decomposition is thus defined by only a single parameter λ, which comprises both the recombination energy and relative mass factors. For HCO^+, Bates calculated λ to be 1.56 for CO in its ground electronic state; in terms of $P(v)$, this means that about 70% of the product CO is vibrationally excited.

The *relic* effect proposed by Bates contains the assumption that the excitation of product CO is derived from multiple vibrational modes in the ion. According to this *relic* model, the C-O coordinate is separated and considered as an independent oscillator. Each normal mode of the ion is characterized by the amplitude it imposes on the C-O distance, so that the wave function for this segregated coordinate is a superposition of vibrations caused by each ground-state normal mode:

$$\Psi_0 = N \sum_{l=1}^{4} \psi_0(\alpha_l |) \exp(i\theta_l) , \tag{7}$$

where $\psi_0(\alpha_l |)$ is the contribution from mode l, α_l is a harmonic oscillator parameter of mode l projected onto the C-O coordinate, N is the normalizing factor, and θ_l is the phase angle coming from an independent time factor for each mode. Then the relative probability of CO being in level v after dissociation is

$$P(v) = Av |\langle \Psi_0 | \psi_v(\alpha |) \rangle| , \tag{8}$$

where $\psi_v(\alpha |)$ is the CO eigenfunction and the average Av is taken over all phase angles. The population of odd levels by the relic mechanism is always zero because for odd v the above overlap integral vanishes.

These mechanisms of Bates (1993) are treated separately so that it is difficult in most instances to compare theory with experimental results. In addition, there is yet another mechanism, not considered by Bates, for product vibrational excitation in which different bond distances in the initial ion and the final product lead to such excitation due to the Franck-Condon principle. In this paper we report a more detailed theoretical approach to the problem that contains both of Bates' effects plus the Franck-Condon mechanism, and we utilize the theory for the dissociative recombination between HCO^+ and electrons.

In our approach the equations of motion are solved starting from the moment in which the system switches from a stable ionic potential to a repulsive neutral one. The efficiency of the curve-crossing is not treated; this efficiency relates to the overall rate coefficient for the process along a given neutral potential surface but not to the product vibrational distribution (Talbi et al. 1989). We follow the dissociation of the neutral HCO molecule along repulsive potential energy surfaces leading to the products H and CO. The dissociation is assumed to occur along a linear trajectory so that the CO cannot become rotationally excited. The equations of motion are solved both classically and quantum mechanically, and the CO product vibrational distribution is calculated. For dissociation into the ground electronic state ($X\,^1\Sigma^+$) of CO, we use a detailed ab initio potential which is newly reported here, whereas for dissociation into the first excited electronic state ($a\,^3\Pi_r$), we use a simple approximate form for the relevant neutral HCO potential. Our results, discussed below, show that the *impulse* mechanism of Bates is responsible for most of the product excitation when CO is produced in its ground electronic state, while the Franck-Condon and *impulse* mechanisms share responsibility for the product excitation when CO is produced in its first excited state. Our vibrational distribution for CO in the latter case is in reasonable but not perfect agreement with experimental measurement (Butler et al. 1998). Regarding the proposal of Duley & Williams (1992), we find that most of the exoergicity of reaction does not go into vibrational energy of CO and subsequent infrared emission.

2. AB INITIO CALCULATIONS

The HCO radical has a strongly bent equilibrium geometry in its ground electronic $\tilde{X}\,^2A'$ state. At linear geometry this state becomes $^2\Pi$ and is degenerate with the first excited $\tilde{A}\,^2A''$ state. The energy splitting between these two states is caused by a strong Renner-Teller coupling. The degenerate $^2\Pi$ state correlates with the excited $a\,^3\Pi$ state of CO, whereas the CO($X\,^1\Sigma^+$) ground state leads to a $^2\Sigma^+$ state of HCO in the linear conformation or in general to $^2A'$. The intersection of the potential of this $^2A'$ state with that of the $\tilde{X}\,^2A'$ ground state arising from the Renner-Teller splitting is avoided. Therefore, in the adiabatic approximation used here, dissociation of the $\tilde{X}\,^2A'$ ground state proceeds via a small potential barrier. At linear geometries, however, the $^2\Sigma^+$ potential determining the linear approach of H(^2S) + CO($X\,^1\Sigma^+$) is entirely repulsive and has a conical intersection with the CH dissociation potential of the degenerate $^2\Pi$ state. The $^2\Sigma^+$ interaction potential was determined here at a high level of ab initio theory for a large number of H-CO separations and for five different CO distances.

The atomic basis sets chosen to approximate the molecular orbitals are of the general contraction type and were constructed according to the atomic natural orbital (ANO) concept (Almlöf & Taylor 1987; Widmark, Malmqvist, & Roos 1990) including the density matrix averaging modification (Widmark et al. 1990). They consist, for carbon and oxygen, of 14 *s*-, 9 *p*-, 4 *d*-, and 3 *f*-type Gaussian functions contracted to (*6s5p3d2f*)-functions and, for hydrogen, of 8 *s*-, 4 *p*-, and 3 *d*-type functions contracted to (*6s3p2d*)-functions; in total 228 primitive functions are contracted to 145 functions.

The energies were evaluated at the multireference configuration interaction (MR-CI) level of theory using molecular orbital bases that were optimized at each geometry point by complete–active-space (CASSCF) calculations (Roos, Taylor, & Siegbahn 1980; Siegbahn et al. 1981; Roos 1980). In the CASSCF partitioning scheme adopted here, the four electrons occupying the carbon and nitrogen 1*s* orbitals were kept inactive, and the remaining 11 valence electrons were allowed to be distributed among eight active orbitals (four σ orbitals and two π_x and π_y orbitals) in all possible ways consistent with the space and spin symmetry of the HCO ($^2\Sigma^+$) state.

In order to avoid prohibitively large expansions in the MR-CI calculations, it was decided here not to use the full CASSCF wave function as a reference state function from which all possible single and double excitations are generated within the available molecular orbital space. The MR-CI reference configuration list was instead restricted to include only those occupations (configuration state functions [CSFs]) for which the absolute value of the coefficient of any of its component spin couplings exceeded a threshold of 0.05 in the CASSCF wavefunctions at any geometry point on the potential surface. The MR-CI reference function constructed in this manner consists of only 15 CSFs. Experience shows that, with this reduced computational approach, rather reliable potential surfaces can be determined with a balanced description of large parts of the surfaces.

Identical calculations were also performed for the $\tilde{X}\,^1\Sigma^+$ ground electronic state potential of the HCO^+ ion for which experimental and accurate theoretical spectroscopic data are available. Dissociation here leads to $H^+ + CO(X\,^1\Sigma^+)$ with an energy separation from the dissociation level of the HCO ground state equal to the ionization energy of hydrogen (13.605 eV). The fact that the present calculations are able to reproduce exactly this number simply shows that the atomic basis set located on the hydrogen center is able to describe the hydrogen (1*s*) electron accurately. Present results for the equilibrium HC distance in HCO^+ ($R_e = 1.091$ Å), the equilibrium CO distance ($R_e = 1.105$ Å), and the proton dissociation energy ($D_e = 6.42$ eV) are also in perfect agreement with the most reliable results in the literature. The shape of the HCO^+ potential at large HC separations is correctly described by the present calculations, in close agreement with the analytical representation of a charge-multipole interaction between the proton and CO. In neutral HCO, on the other hand, the induction forces between H and CO are so weak that the potential is entirely repulsive with a shallow energy barrier occurring for bent geometries on the global $\tilde{X}\,^2A'$ potential, which is due to an avoided surface intersection, as discussed above. At short H-C separations, the repulsive HCO potential approaches the minimum region of the ionic HCO^+ potential and, in the adiabatic approximation, the eigenfunctions obtained in the MR-CI calculations gain Rydberg character. As a result, the potential in this region shows a slight deformation and becomes identical with the potential of the lowest Rydberg state of $^2\Sigma^+$ symmetry at shorter H-C distances, as has already been found previously (Tanaka & Davidson 1979).

In order to assess the reliability of the binding characteristics in the CO fragment provided by the present calculations, the lower part of the CO potential was determined with the same level of ab initio theory, and the spectroscopic constants were evaluated. A few comparisons with the corresponding experimental data given in parentheses (Huber & Herzberg 1979) demonstrate the quality of the theoretical approach applied in this study: $R_e = 1.131$ Å (1.1283 Å), $\omega_e = 2176$ cm^{-1} (2169.81 cm^{-1}), $\omega_e x_e = 14.6$ cm^{-1} (13.29 cm^{-1}), $B_e = 1.92$ cm^{-1} (1.9313 cm^{-1}), and $\alpha_e = 0.016$ cm^{-1} (0.0175 cm^{-1}). We conclude that the *ab initio* description of the very limited part of the global HCO ($\tilde{X}\,^2A'$) potential surface required for the dynamical calculations of this study can be expected to be rather reliable. In the dynamical calculations described below, the surface is represented by a spline procedure.

All the ab initio calculations were performed using the MOLCAS-3 suite of programs (Andersson et al. 1994). Extensions of these calculations to the lowest excited $^2\Pi$ and $^2\Sigma^+$ states of HCO are in progress.

3. MODEL

In our model we assume that the HCO^+ ion is not rotationally excited and lies in its ground vibrational state. We further assume that electron capture does not change the instantaneous vibrational motion of the atoms, so that in the quantum mechanical calculations the initial HCO neutral wave function is that of the ion (subject to one change in equilibrium bond distances discussed below). For simplicity, dissociation is assumed to occur along a collinear path only, so that the problem reduces to a determination of the H-C and C-O distances as a function of time as dissociation occurs into H and CO on a repulsive neutral surface.

The calculated ground state HCO potential (see § 2), which correlates with CO $(X\,^1\Sigma^+) + H$, is depicted in Figure 1 for linear configurations as a function of H-C distance with the CO distance adjusted for minimum energy. The ionic potential surface is also depicted. The CO distance used changes a negligible amount from the equilibrium distance in the HCO^+ ion to that in the CO molecule in its ground electronic state. Because the transfer from ionic to neutral potential curve occurs at the potential energy of the HCO^+ ion at its equilibrium position, it cannot occur directly with high probability because, as can be seen in the figure, the two curves do not intersect at the equilibrium bond distances. We assume for simplicity that the transfer occurs at a shorter H-C distance, specifically that distance where the two curves cross with CO held to its equilibrium distance in the ion. Rather than using that small portion of the HCO^+ vibrational wave function at this distance, we shift the equilibrium H-C distance in the HCO^+ vibrational wave function (see Fig. 1), thus making the direct curve crossing more efficient than it should be. This assumption can be made because we are not interested in the total efficiency of the process but in the vibrational

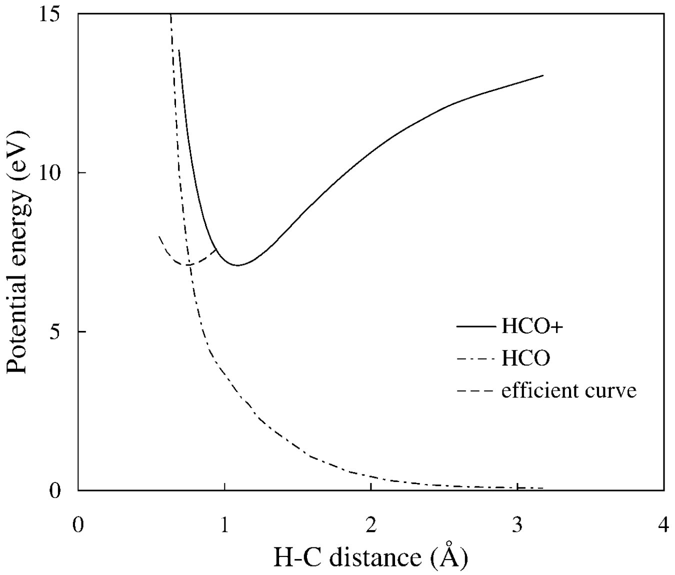

FIG. 1.—Potential energy of the ground state of the HCO^+ ion and of the repulsive $^2\Sigma$ state of the HCO neutral are plotted vs. the H-C bond distance with the C-O bond distance adjusted for minimum neutral state energy. In our calculations the equilibrium H-C value of the ionic curve is moved to smaller distances, as shown, so that curve crossing occurs with zero kinetic energy in the H-C bond.

distribution of the CO product. Any immediate CO excitation at this stage due to some multistep indirect mechanism is neglected. According to the indirect mechanism (Bates 1993), during the first stage of dissociation the system falls down to lower Rydberg states that lie closer to the neutral dissociative curve, allowing the decomposition to proceed. The effect of our neglect of some initial CO excitation is unclear, but obviously leads to a lower limit for the CO product vibrational excitation.

To help gauge the effect of a direct curve crossing at a short H-C bond distance, we have also used a simple analytical potential for the ground state of HCO that passes through the minimum of the ionic potential surface. This potential is of the form

$$V_\Sigma(\xi, R) = \frac{\mu_R \omega_{\mathrm{CO}}^2 (R - R_{\mathrm{CO}})^2}{2} + E_0 \exp\left(-\frac{\xi - \xi_{\mathrm{HCO^+}}}{\sigma}\right), \tag{9}$$

where ξ is the H-C internuclear distance, R is the CO internuclear distance, μ_R is the CO reduced mass, and ω_{CO} is the angular harmonic frequency of CO, while $E_0 = 7.3$ eV is defined so that the neutral curve reaches the ionic curve at its equilibrium configuration, assuming no change in the CO equilibrium distance ($R = R_{\mathrm{CO}}$, $\xi = \xi_{\mathrm{HCO^+}}$). The parameter σ was set to 0.31 Å by comparing V_Σ with the newly calculated ab initio potential as well as a previously calculated one (Talbi et al. 1989). The actual potential surfaces are steeper than V_Σ at small H-C distances and flatter at large ones.

To study the dissociation of HCO leading to CO in its excited $a\ ^3\Pi_r$ electronic state, we used a simplified analytical HCO potential denoted by $V_\Pi(\xi, R)$ and based on thermodynamic and spectroscopic parameters. A major difference between V_Σ and V_Π is that as HCO dissociates into the excited state of CO, there is large change in the CO distance and harmonic frequency. The latter changes from 2170 cm^{-1} (the HCO^+ value) to 1740 cm^{-1} in the $a\ ^3\Pi_r$ state, while the bond distance changes from 1.105 to 1.209 Å. To model this change, we used a simple switching function potential:

$$V_\Pi(\xi, R) = V_{\mathrm{HCO^+}}(R)[1 - \tanh x] + V_{\mathrm{CO}}(R) \tanh x + E_0' \exp\left(-\frac{\xi - \xi_{\mathrm{HCO^+}}}{\sigma_2}\right), \tag{10}$$

where

$$x = \max\left(\frac{\xi - \xi_{\mathrm{HCO^+}}}{\sigma_1}, 0\right) \tag{11}$$

is the switching parameter. This potential intersects the ionic potential at its equilibrium point, as does V_Σ. The parameter $E_0' = 1.3$ eV, taking into account the electronic energy of the $a\ ^3\Pi_r$ state, while the parameters σ_1 and σ_2 are set to a value of 0.3, which is close to the value used for the ground-state analytical potential.

The dissociation of HCO into H and CO has been followed both classically and quantum mechanically. To solve the classical equations of motion, a standard fourth-order Runge-Kutta method was used. Trajectories were followed with a time step of 0.001 fs (1×10^{-18} s) until the H atom was 5–6 Å distant from the C atom. Then the CO vibrational energy was calculated and binned into the closest vibrational level. In the case of the analytic potential, a simple harmonic oscillator approximation for the C-O coordinate was used, and the vibrational level v was calculated from the energy E in this coordinate by

$$v = \left\lfloor \frac{E}{\hbar \omega_{\mathrm{CO}}} \right\rfloor, \tag{12}$$

where the symbol $\lfloor \ldots \rfloor$ refers to the integer part of the floating point number. For the ab initio potential, the vibrational levels of CO vibrational are not equally spaced. Therefore, their energies were calculated beforehand, and the final vibrational state of CO was assigned in accordance with the closest level in the CO spectrum.

To solve the quantum mechanical problem, direct integration of the time-dependent Schrödinger equation

$$i\hbar \frac{\partial \Psi(r, R, t)}{\partial t} = \left[-\frac{\hbar^2}{2\mu_r}\frac{\partial^2}{\partial r^2} - \frac{\hbar^2}{2\mu_R}\frac{\partial^2}{\partial R^2} + V(r, R)\right]\Psi(r, R, t) \tag{13}$$

was utilized, where the coordinate r is defined by

$$r = \xi + \frac{m_{\mathrm{O}}}{m_{\mathrm{C}} + m_{\mathrm{O}}} R, \tag{14}$$

while

$$\mu_r = \frac{m_{\mathrm{H}}(m_{\mathrm{C}} + m_{\mathrm{O}})}{(m_{\mathrm{H}} + m_{\mathrm{C}} + m_{\mathrm{O}})}. \tag{15}$$

Both r and the reduced mass μ_r relate to the motion between H and the CO center of mass.

Integration was accomplished by using the discrete variable representation (DVR) (Muckerman 1990). The coordinate R, which is involved only in bounded oscillational motion, does not change significantly and was described by employing a DVR basis set composed of harmonic oscillator eigenfunctions with adjusted weights w_j and quadrature points x_j:

$$u_j(x) = \frac{w_j}{\sqrt{\pi}} \exp\left(-\frac{x^2 + x_j^2}{2}\right) \sum_{n=0}^{N-1} \frac{1}{2^n n!} H_n(x) H_n(x_j), \tag{16}$$

with

$$x = \left(\frac{\mu_R \omega_{\mathrm{CO}}}{\hbar}\right)^{1/2} (R - R_0). \tag{17}$$

The center of the gridpoint region R_0 was chosen to be the average of the equilibrium R distance in HCO^+ and that in the CO molecule. The number of gridpoints $N = 10$ proved to be quite sufficient to cover all accessible R values.

For the r coordinate, along which dissociation occurs, we used a simple periodic DVR (Muckerman 1990),

$$u_j(x) = \frac{w_j}{2\pi} \sum_{n=1}^{N} \cos\left[k_n(x - x_j)\right], \quad -\pi \le x \le \pi \tag{18}$$

with equally spaced gridpoints x_j and equal weights w_j:

$$x_j = \frac{(2j - N - 1)\pi}{N}, \quad k_n = \frac{(2n - N - 1)}{2}, \quad w_j = \frac{2\pi}{N}, \tag{19}$$

where the indices j and n range from 1 to N. The domain of the variable r was mapped onto the $[-\pi, \pi]$ interval by

$$x = \pi \frac{2r - (r_{\max} + r_{\min})}{r_{\max} - r_{\min}} , \quad r_{\min} \le r \le r_{\max} . \qquad (20)$$

The domain of u_j in terms of r needs to be broad enough for the time-dependent wave function to be accurately produced until vibrational distribution in CO is established. As our calculations revealed, the final vibrational population is completely reached by $t \sim 10$ fs when r is about 4.5 Å. For all calculations the interval from $r_{\min} = 0.5$ Å to $r_{\max} = 8.5$ Å was used.

Dissociation into the CO ground $X\,^1\Sigma^+$ state produces products with a significant ($\approx$7 eV) amount of kinetic energy in the H-C coordinate and requires the use of a sufficiently dense gridpoint net. We used $N = 400$ for dissociation into the ground state and $N = 200$ for dissociation into the excited $a\,^3\Pi_r$ state. These numbers were varied to ensure their adequacy.

As the dissociation occurs, the population of CO vibrational level v can be calculated via the superposition principle at specific times and distances r:

$$\Psi(r, R, t) = \sum_v a_v(r, t)\psi_v(R) , \qquad (21)$$

$$P(v) = |a_v|^2 , \qquad (22)$$

where $\Psi(r, R, t)$ is the system wave function, and $\psi_v(R)$ is the vibrational wave function for level v. In our tabulated results, we have integrated the results for $P(v)$ over all distances r since the system wave function is spread out in this coordinate at any time t.

4. RESULTS

Table 1 shows our calculated fractional populations for CO $X\,^1\Sigma^+$ as a function of vibrational state v along with results obtained from the *impulse* and *relic* mechanisms of Bates (1993). In addition we tabulate the fraction of the CO population in excited vibrational states ($v > 0$) and the average energy in vibration. Our calculated values for CO(v) are listed according to the type of calculation (DVR, classical trajectory) and to the HCO potential used (ab initio, analytical). Selected CO fractional populations are also shown in Figure 2.

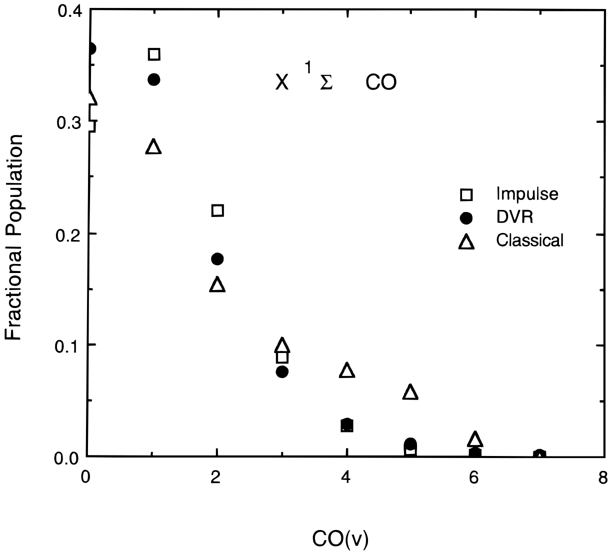

FIG. 2.—Fractional populations of product CO in its ground electronic state as a function of vibrational state. Shown are the results of the *impulse*, DVR, and classical calculations for the dissociative recombination of HCO$^+$ + e. The latter two sets of results are based on the ab initio potential.

It can be seen that the type of potential used and the type of calculation undertaken do not strongly affect the results; all of our calculations show $\approx$65%–70% of the CO product in excited vibrational states with the average vibrational energy 0.4–0.6 eV. Note that most of the reaction exoergicity goes into H + CO relative translational energy and not into vibration, contrary to the suggestion of Duley & Williams (1992). (Since we are doing collinear calculations, no energy can go into rotational excitation of CO.) Our results also show that the CO vibrational population is established rather early in the reaction. In Figure 3 we plot calculated CO vibrational populations as functions of the H-CO coordinate r for the dissociation into the ground state, obtained by using the DVR method with the ab initio potential. In terms of time, it takes only $\approx$2 fs for vibrational levels to adjust their population to near final results; this period of time is much less than the CO vibrational period of 15 fs.

Our calculated CO vibrational distributions are in excellent agreement with the simple *impulse* mechanism of Bates (1993). This is not surprising since (1) the equilibrium CO distance is almost the same in the HCO$^+$ ion and the $X\,^1\Sigma^+$ state so that Franck-Condon effects are not important, and (2) dissociation occurs quickly compared to the CO vibrational period. The *relic* mechanism of Bates does not appear to play an important role. Both our approach and the *impulse* mechanism do not include an initial CO excitation, as might occur in a multistep indirect curve-crossing from the ionic to the neutral potential surface.

TABLE 1

VIBRATIONAL STATE POPULATION FOR CO $X\,^1\Sigma^+$

	v								
METHOD	0	1	2	3	4	5	6	FRACTION ($v > 0$)	$\langle E_{\mathrm{vib}} \rangle$ (eV)
Impulse	0.296	0.360	0.219	0.089	0.027	0.007	0.001	0.70	0.46
Relic	0.78	0	0.12	0	0.06	0	0.03	0.22	0.34
DVR									
ab initio......	0.365	0.337	0.178	0.075	0.029	0.011	0.004	0.63	0.43
V_Σ............	0.359	0.359	0.188	0.068	0.020	0.005	0.001	0.64	0.41
Classical[a]									
ab initio......	0.322	0.278	0.155	0.100	0.077	0.058	0.017	0.68	0.56
V_Σ............	0.364	0.310	0.189	0.129	0.009	0.000	0.000	0.64	0.43

[a] Based on 10000 trajectories.

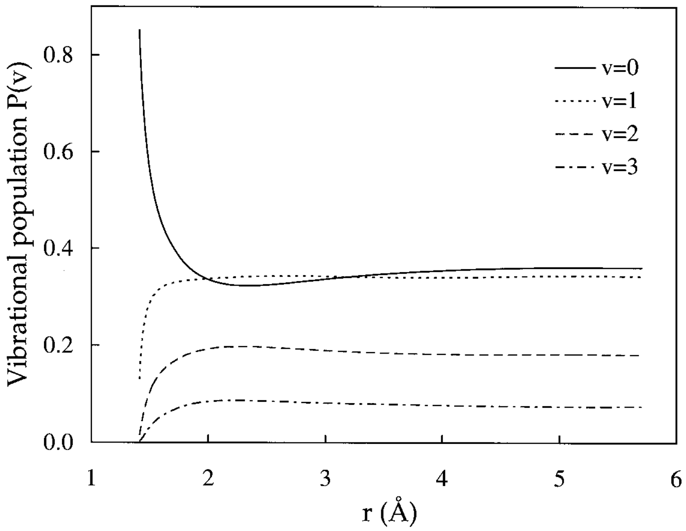

FIG. 3.—Fractional populations for vibrational states of product CO in its ground electronic state plotted against the coordinate r, which is the distance between H and the center of mass of CO. The values derive from the DVR calculation with the ab initio potential.

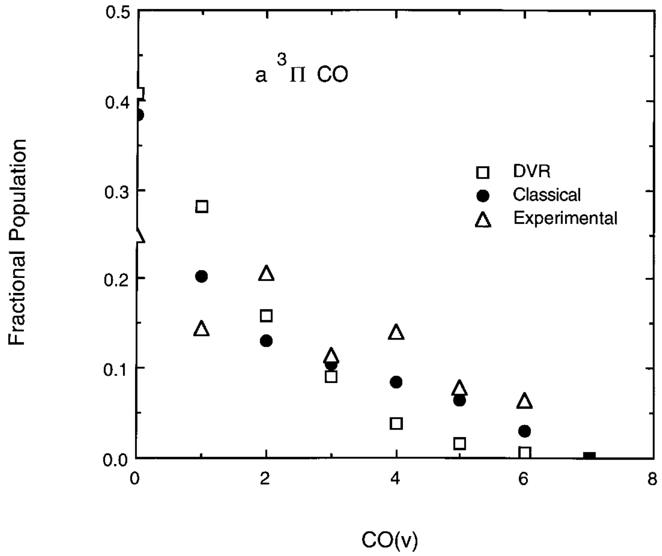

FIG. 4.—Fractional populations of product CO in its first excited (a) electronic state as a function of vibrational state. Shown are the experimental results of Adams & Babock (1994) as well as the results of DVR and classical calculations for HCO$^+$ + e.

Table 2 and Figure 4 show the analogous quantum and classical calculated CO(v) fractional populations for the CO $a\ ^3\Pi_r$ state along with the experimental data of Adams & Babcock (1994) and Butler et al. (1997). Table 2 also contains results obtained from the *impulse* mechanism. The *impulse* mechanism leads to much less excitation than for the CO ($X\ ^1\Sigma^+$) case since the reaction exoergicity leading to CO in its $a\ ^3\Pi_r$ state is only 1.3 eV compared with 7.3 eV for the CO ground electronic state. Our classical and quantum results, obtained with a simple analytical potential (V_Π), show much more vibrational excitation than does the *impulse* mechanism because there is a large change in the CO equilibrium separation between the HCO$^+$ ion (1.105 Å) and the a state (1.209 Å), leading to a Frank-Condon–type excitation effect. The *relic* mechanism of Bates is inapplicable to the production of $a\ ^3\Pi_r$ CO because of the large change in bond distance.

Our classical result (62% excitation) shows slightly more vibrational excitation than does the quantum calculation (59% excitation). Both show somewhat less excitation than do the tabulated experimental results of Adams & Babcock (1994; 75% excitation) and somewhat more excitation than the more recent experimental results of Butler et al. (1997; 47% excitation). We note that changing the parameters σ_1 and σ_2 used in the potential in the range 0.2 to 0.4 Å does not affect the population of the higher vibrational levels of CO strongly. We hope to eventually have an *ab initio* potential for HCO dissociation into H and CO ($a\ ^3\Pi_r$).

In the interstellar medium, formation of CO in its metastable $a\ ^3\Pi_r$ state would be followed by radiative relaxation of the CO into its ground electronic state with the concomitant emission of ultraviolet radiation. The initial vibrational population in the excited electronic state would be changed following relaxation due to nondiagonal Franck-Condon

TABLE 2

VIBRATIONAL STATE POPULATION FOR CO $a\ ^3\Pi_r$

METHOD	v							FRACTION ($v > 0$)	$\langle E_{\rm vib} \rangle$ (eV)
	0	1	2	3	4	5	6		
HCO$^+$ + e^- → H + CO ($a\ ^3\Pi$)									
Impulse	0.743	0.220	0.033	0.003	0.000	0.000	0.000	0.26	0.17
DVR	0.407	0.280	0.158	0.090	0.039	0.016	0.007	0.59	0.35
Classical[a]	0.383	0.202	0.129	0.103	0.085	0.066	0.031	0.62	0.46
Experiment[b]	0.25	0.15	0.21	0.12	0.14	0.078	0.065	0.75	0.59
Experiment[c]	0.53	0.17	0.091	0.085	0.085	0.014	0.022	0.47	0.35
DCO$^+$ + e^- → D + CO ($a\ ^3\Pi$)									
Impulse	0.576	0.318	0.088	0.016	0.002	0.000	0.000	0.42	0.23
DVR	0.509	0.320	0.130	0.032	0.007	0.001	0.000	0.49	0.26
Classical[a]	0.461	0.197	0.129	0.105	0.100	0.008	0.000	0.53	0.37
Experiment[c]	0.53	0.17	0.091	0.085	0.085	0.014	0.022	0.47	0.35

[a] Based on 10000 trajectories.

[b] Adams & Babcock 1994.

[c] Butler, Babcock, & Adams 1997; these data, presented only in a figure, differ somewhat from the earlier data for HCO$^+$. The more recent data appear to show less vibrational excitation and are in closer agreement with our calculated results.

factors. Since the change in vibrational energy can be both positive and negative, one would not expect a great change in the average amount of vibrational excitation (≈ 0.5 eV). Therefore, despite the fact that the *a* state lies so much higher in energy than the ground electronic state of CO, most of the energy radiated away, as CO initially produced in the *a* state cools to the temperature of the cloud, will not be in the infrared, contrary to the suggestion by Duley & Williams (1992).

It would appear therefore that the vibrational excitation is only moderate whether CO is produced directly in its ground state or initially in its first excited state followed by radiative relaxation to its ground state. Of course, we currently do not know the fraction of product CO in its ground state and in its first excited (*a*) electronic state. Such a determination by theoretical means will require knowledge of the ionic to neutral curve crossing efficiencies for the two neutral repulsive surfaces.

Since Butler et al. (1997) have also measured the vibrational distribution of product CO in its $a\ ^3\Pi_r$ state following the dissociative recombination of DCO^+, we have calculated the distribution as well and listed our results in Table 2 along with the measured distribution and that obtained via the *impulse* method. The experimental result, that there is no difference between the CO(v) distribution for $HCO^+ + e$ and for $DCO^+ + e$, is not reproduced by the calculations. With the *impulse* mechanism, the calculated degree of vibrational excitation for $DCO^+ + e$ exceeds that for $HCO^+ + e$, rising from 26% to 42%. The increase occurs because the departing deuterium atom causes a greater effect on the C-O bond than does the departing hydrogen atom. Both our detailed classical and quantum calculations show less vibrational excitation for $DCO^+ + e$ than for $HCO^+ + e$, although they still produce greater vibrational excitation than does the *impulse* mechanism. The level of agreement between our detailed calculations and the experimental results is comparable to that for $HCO^+ + e$, with the exception of the highest vibrational state studied in the experiment ($v = 6$).

5. DISCUSSION

Our calculations show that a significant but not dominant amount of energy in the dissociative recombination of HCO^+ goes into vibrational excitation of the CO product. For CO formed in its ground (X) state, our detailed calculations show that, on average, $\approx$0.4–0.6 eV goes into vibration while the remainder of the energy, $\approx$7.0 eV, goes into relative translational energy between H and CO. The small fraction in vibrational energy is in qualitative agreement with the view of Talbi et al. (1989). For CO formed in its excited *a* state, our calculated vibrational distribution, based only on a simple analytical form for the repulsive HCO potential surface, shows somewhat less excitation than the experimental results of Adams & Babcock (1994) and somewhat more excitation than the later experimental results of Butler et al. (1997). The average energy in vibration, $\approx$0.5 eV, will roughly be preserved in the low-density interstellar medium as the CO undergoes the electronic transition $a \rightarrow X$. Thus, the amount of vibrational energy that can be converted into infrared radiant energy in the interstellar medium is not a major fraction of the total energy available whether the CO is formed in its ground state or in its first excited electronic state. The chances of detecting this infrared radiation are considerably smaller than if most of the exoergicity of reaction were convertible into infrared emission.

Eric Herbst would like to acknowledge the National Science Foundation for support of his research in astrochemistry. He is also grateful to the Ohio Supercomputer Center for computer time on their Cray Y-MP/8.

REFERENCES

Adams, N. G. 1992, in Advances in Gas Phase Chemistry, Vol. 1, ed. N. G. Adams & L. M. Babcock (Greenwich: JAI Press), 271
Adams, N. G., & Babcock, L. M. 1994, ApJ, 434, 184
Adams, N. G., et al. 1991, J. Chem. Phys., 94, 4852
Adams, N. G., & Smith, D. 1988, in Rate Coefficients in Astrochemistry, ed. T. J. Millar & D. A. Williams (Dordrecht: Kluwer), 173
Almlöf, J., & Taylor, P. R. 1987, J. Chem. Phys., 86, 4070
Anderson, K. et al. 1994, MOLCAS-3 Suite of Programs, Technical Rep., Univ. of Lund, Sweden
Bates, D. R. 1993, MNRAS, 263, 369
Butler, J. N., Babcock, L. M., & Adams, N. G. 1997, Mol. Phys, 91, 81
Duley, W. W., & Williams, D. A. 1992, MNRAS, 257, 13P
Herbst, E. 1995, Ann. Rev. Phys. Chem., 46, 27
Herd, C. R., Adams, N. G., & Smith, D. 1990, ApJ, 349, 388
Huber, K. P. & Herzberg, G 1979, Molecular Spectra and Molecular Structure, IV. Constants of Diatomic Molecules (New York: van Nostrand)
Larsson, M., Lepp, S., & Dalgarno, A. 1996, A&A, 309, L1
Mitchell, J. B. A. 1990, Phys. Rep., 186, 215
Muckerman, J. T. 1990, Chem. Phys. Lett., 173, 202
Roos, B. O. 1980, Int. J. Quantum Chem. Symp, 14, 175
Roos, B. O., Taylor, P. R., & Siegbahn, P. E. M. 1980, Chem. Phys., 48, 157
Siegbahn, P. E. M., Almlöf, J., Heiberg, A., & Roos, B. O. 1981, J. Chem. Phys., 74, 2384
Talbi, D. Hickman, A. P., Pauzat, F., Ellinger, Y., & Berthier, G. 1989, ApJ, 339, 231
Tanaka, K, & Davidson, E. R. 1979, J. Chem. Phys., 70, 2904
Vejby-Christensen, L., Andersen, L. H., Heber, O., Kella, D., Pedersen, H. B., Schmidt, H. T., & Zaifman, D. 1997, ApJ, 483, 531
Widmark, P.-O., Malmqvist, P.-Å, & Roos, B. O. 1990, Theor. Chim. Acta, 77, 91
Williams, T. L., Adams, N. G., Babcock, L. M., Herd, C. R., & Geoghegan, M. 1996, MNRAS, 282, 413